Balance Control and Analysis of Stationary Riderless Motorcycles

Yizhai Zhang, Jingliang Li, Jingang Yi, and Dezhen Song

Abstract— **We present balancing control analysis of a stationary riderless motorcycle. We first present the motorcycle dynamics with an accurate steering mechanism model with consideration of lateral movement of the tire/ground contact point. A nonlinear balance controller is then designed. We estimate the domain of attraction (DOA) of motorcycle dynamics under which the stationary motorcycle can be stabilized by steering. For a typical motorcycle/bicycle configuration, we find that the DOA is relatively small and thus balancing control by only steering at stationary is challenging. The balance control and DOA estimation schemes are validated by experiments conducted on the Rutgers autonomous motorcycle. The attitudes of the motorcycle platform are obtained by a novel estimation scheme that fuses measurements from global positioning systems (GPS) and inertial measurement units (IMU). We also present the experiments of the GPS/IMU-based attitude estimation scheme in the paper.**

I. Introduction

Single-track vehicles such as motorcycles and bicycles is underactuated and intrinsically unstable. As shown in [1], the motorcycle/bicycle systems become much easier to be stabilized at a faster moving velocity. When a riderless motorcycle is at stationary, namely, zero moving velocity, balancing by only steering actuation becomes extremely challenging. The main objective of this paper is to present an analysis of balance control of stationary riderless motorcycle with only front-wheel steering control.

Motorcycle dynamics and stability are studied extensively and the modeling work can be considered as two groups [2], [3]: simple inverted pendulum models and multi-body dynamic models. Most of these dynamic models consider either riderless motorcycle/bicycle systems [1], [4]–[8], or simple human/bicycle interaction dynamics [9], [10]. Stability characteristics are typically discussed using a linearization approach with consideration of a constant velocity [1]–[3], [11], [12]. Control of a riderless autonomous motorcycle/bicycle has also been proposed in [6], [13]–[17]. Most of these autonomous systems use both steering and traction/braking as control actuation except that in [13], [14], additional actuation such as weight-shifting or gyroscopic forces are used to balance the systems.

This work was partially supported by the National Science Foundation under CAREER award CMMI-0954966 (J. Yi).

Y. Zhang and J. Yi are with the Department of Mechanical and Aerospace Engineering, Rutgers University, Piscataway, NJ 08854 USA. E-mail: yzzhang@eden.rutgers.edu (Y. Zhang) and jgyi@rutgers.edu (J. Yi).

J. Li is with the School of Mechanical and Vehicular Engineering, Beijing Institute of Technology, Beijing 100081, P. R. China (e-mail: lijingliang@bit.edu.cn). This work was conducted when J. Li was a visiting Ph.D. student at Rutgers University.

D. Song is with the Department of Computer Science and Engineering, Texas A&M University, College Station, TX 77843 USA. E-mail: dzsong@cse.tamu.edu

Balancing control of a stationary riderless motorcycle is the main topic of this work. Here we consider front-wheel steering as the only control actuation of the system. The motivation for this study is twofold. First, balance control of stationary motorcycle systems is much more challenging than that under a certain velocity. With only steering control, we show that the balance is maintained within a certain dynamic region. We reveal and explicitly identify this attraction region. If the motorcycle state is outside this region, it is impossible to maintain balance only by steering and some other control mechanisms (e.g., weight shifting) are needed. Second, understanding the balance capability by only steering is important for practical applications such as the use of bicycle systems as rehabilitation device for recovering human postural control for disabilities patients [18].

The dynamics of the stationary motorcycle systems are conceptually similar to two-link coupled inverted pendulums. However, the complexity of the motorcycle dynamics comes from the interconnected multi-body mechanisms. The balance of the platform by steering control is obtained through the movement of the center of the gravity of the system. We reveal and experimentally test the relationship between steering and the height change of the motorcycle center of gravity. To analyze and estimate the domain of attraction (DOA) of the motorcycle dynamical systems, we extend the approach in [19] with consideration of steering mechanism for the motorcycle systems under a sliding-mode stabilization controller. We also demonstrate a novel attitude estimation scheme by fusing the position information from global positioning systems (GPS) with measurements from onboard low-cost inertial measurement units (IMU).

The remainder of the paper is organized as follows. In Section II, we discuss motorcycle models. In Section III, we present the balancing control and the DOA analysis for the stationary motorcycle system. We present the GPS/IMU attitude estimation scheme in Section IV. Experimental setup and results are presented in Section V. Finally, we conclude the paper in Section VI.

II. Motorcycle Dynamics

A. Steering mechanism and geometric relationships

Fig. 1(a) shows the Rutgers autonomous motorcycle system. The values of the motorcycle physical parameters are listed in Table I. From the geometry of the front wheel steering mechanism [8], we find the following relationship.

$$\tan\beta_g \, \mathrm{c}_\phi = \tan\beta \, \mathrm{c}_\xi, \tag{1}$$

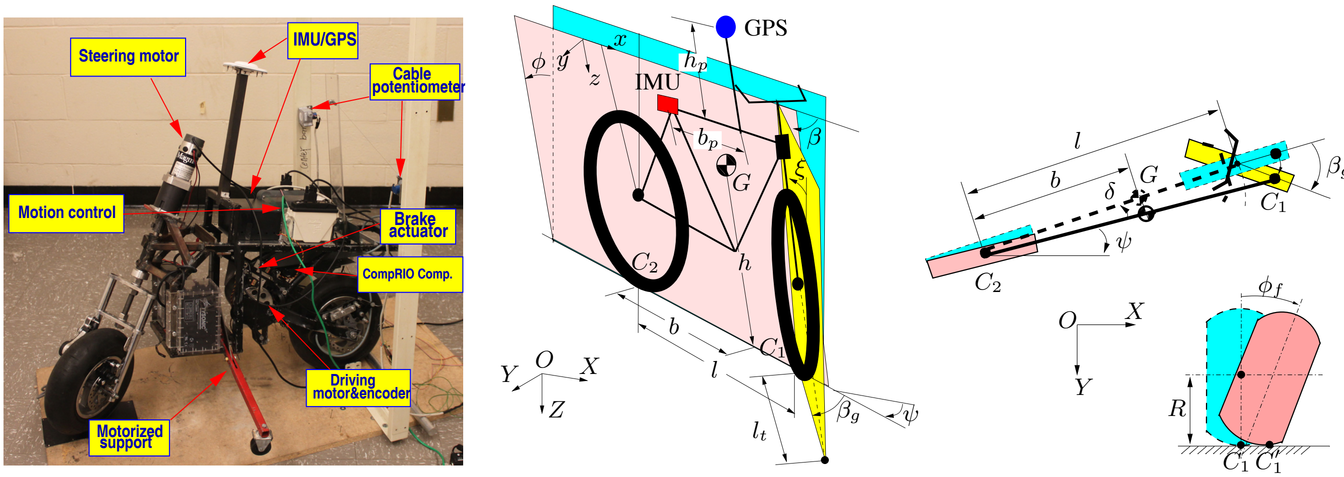

(a) (b) (c)

Fig. 1. (a) Rutgers autonomous motorcycle system. (b) Schematic of the motorcycle system. (c) Top view of the steering mechanism and the front tire geometry under steering.

where we use notations $c_\phi := \cos\phi$ and $s_\phi := \sin\phi$ for roll angle ϕ and other angles, ξ is caster angle, β and β_g are steering angle and projected steering angle, respectively. To facilitate the explanation of the influence of the steering mechanism on motorcycle stability, we first assume that the front tire rotates about the fixed axis; see Fig. 1(c). Due to the steering mechanism and a caster angle ξ, the height change Δh_G of the center of gravity G is calculated by an estimate of the motorcycle frame rotation angle δ. In [8], lateral deflection angle δ of the rear frame is approximated as

$$\delta = \frac{l_t\, c_\xi}{l}\beta_g, \tag{2}$$

where l is the wheel base and l_t is the wheel trail. The height change Δh_G is then calculated by the following equation

$$\Delta h_G(\beta,\phi) = \delta b\, s_\phi = \frac{b l_t\, s_\phi\, c_\xi}{l}\beta_g, \tag{3}$$

where b is the horizontal distance between the rear tire/ground contact point C_2 and the mass center G.

The formulation (3) does not consider the movement of the tire/ground contact point C_1. Fig. 2 illustrates the steering mechanism geometry. As shown in the figure, because the front wheel plane moves from Π_s to Π_s', the height of the center of gravity G is changed from two sources. The first one is the change of height of front tire center point (from O_f to O_f'). We denote the height difference between O_f and O_f' as Δh_{O_f}. The second source comes from the lateral movement of C_1 (to C_1'). We denote the lateral movement distance between C_1 and C_1' as Δy_{c_1}. In the following, we first discuss how to compute Δh_{O_f} and Δy_{c_1} and then revise the formulation of Δh_G in (3).

We assume that under steering point C_1 is moving on a circular curve with radius R which contains the effect of tire width. Notice the fact that if the steering angle is 90 degs, the arc length of curve $\widehat{C_1 C_1'}$ is equal to $R\xi$ [8]. In this special case, $\beta_g = \frac{\pi}{2}$ and it is straightforward to calculate that $\Delta h_{O_f} = R(1-\cos\xi)$. For any general steering angle β_g, we approximate Δh_{O_f} proportionally to that of the special case of $\beta_g = \frac{\pi}{2}$. Therefore, we obtain

$$\Delta h_{O_f} = R\left[1-\cos\left(\frac{\beta_g}{\pi/2}\xi\right)\right] = R\left[1-\cos\left(\frac{2\beta_g\xi}{\pi}\right)\right].$$

Then, we approximate the height change of G as

$$\Delta h_{G1} = R\cos\phi\left[1-\cos\left(\frac{2\beta_g\xi}{\pi}\right)\right]\frac{b}{l}. \tag{4}$$

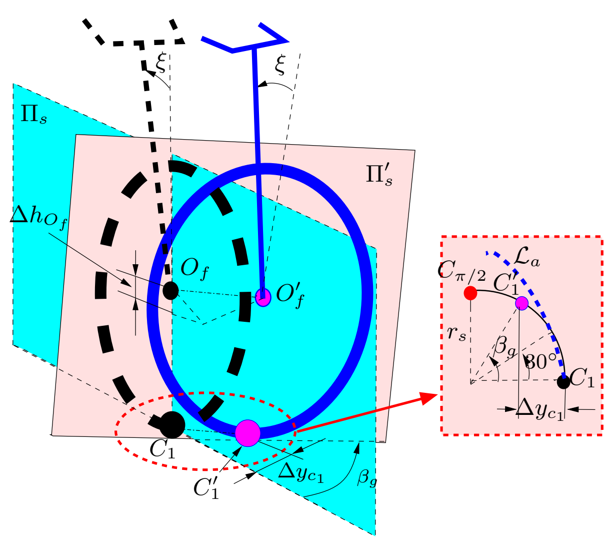

Fig. 2. Schematic of the front wheel steering mechanism.

To calculate Δy_{c_1}, we take the similar approach as Δh_{O_f}. We illustrate the calculation in Fig. 2. We denote the contact point as $C_{\pi/2}$ under steering angle $\beta_g = \frac{\pi}{2}$. We assume that the trajectory of $C_1C_{\pi/2}$ is a circular curve with radius $r_s = \frac{R\xi}{\pi/2}$ (since the moving length from C_1 to $C_{\pi/2}$ is $R\xi$ by the definition of the caster angle ξ). We approximate Δy_{c_1} proportionally to that of steering angle is $\pi/6$, namely,

$$\frac{\Delta y_{c_1}}{\beta_g} = \frac{r_s\,(1-\cos\pi/6)}{\pi/6}$$

TABLE I

MOTORCYCLE PARAMETERS

m (kg)	b (m)	l (m)	l_t (m)	h (m)	ξ (deg)	R (m)	I_x (kgm^2)	b_p (m)	h_p (m)
34.9	0.34	0.74	0.05	0.27	31	0.15	1.8	0.038	0.34

The above calculation is illustrated in Fig. 2 by assuming that the lateral displacement of C_1' is proportional to that of $\beta_g = \frac{\pi}{6}$. By such an approximation, we obtain

$$\Delta y_{c_1} = \frac{12R\xi}{\pi^2}\left(1 - \cos\frac{\pi}{6}\right)\beta_g. \tag{5}$$

We here choose $\beta_g = \frac{\pi}{6}$ as the reference point mainly for simplicity to obtain a linear relationship between Δy_{c_1} and β_g. Note that by considering the lateral movement of point C_1, we need to deduct an angle of magnitude $\frac{\Delta y_{c_1}}{l}$ from δ in (2) to revise the calculation of Δh_G in (3).

Using the above discussions with (4) and (5), we revise the relationship in (3) as follows

$$\begin{aligned}\Delta h_G(\beta, \phi) &= \left(\delta - \frac{\Delta y_{c_1}}{l}\right) b\,\mathrm{s}_\phi - \Delta h_{G1} \\ &= \frac{b l_t\,\mathrm{c}_\xi\,\mathrm{s}_\phi}{l}\beta_g - \frac{12Rb\xi\,\mathrm{s}_\phi}{\pi^2}\left(1 - \cos\frac{\pi}{6}\right)\beta_g \\ &\quad - \frac{bR\,\mathrm{c}_\phi}{l}\left[1 - \cos\left(\frac{2\xi\beta_g}{\pi}\right)\right]. \end{aligned} \tag{6}$$

Fig. 3 shows that the new model is much more accurate than the linear approximation model (3).

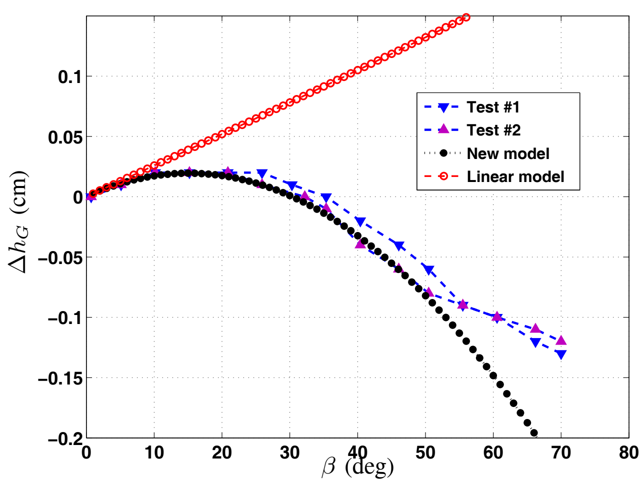

Fig. 3. Experimental comparison of Δh_G with different model predictions with initial roll angle $\phi = -3.8°$.

B. Motorcycle dynamics

Similar to our previous study [15], [20], we use the Lagrangian equations to obtain the dynamic equation of the motion of a stationary riderless motorcycle. We obtain the dynamics equation as follows

$$\ddot{\phi} = \frac{mg\sin\phi}{I_x + mh^2}\left(h + \frac{\alpha R b}{l}\right) + \frac{mgb\,\mathrm{c}_\phi}{(I_x + mh^2)l}\left[l_t\,\mathrm{c}_\xi - \frac{12R\xi}{\pi^2}\left(1 - \frac{\sqrt{3}}{2}\right)\right]\beta_g, \tag{7}$$

where $\alpha := 1 - \cos\left(\frac{2\xi\beta_g}{\pi}\right)$, m is the total mass of the motorcycle system, h is the height of mass center G, I_x is the mass moment of inertia of the motorcycle system along the x-axis, and g is the gravitational constant. Due to the page limit, we neglect the detailed derivation of (7) and readers can refer to the similar derivations in [15], [20].

III. BALANCE STABILITY AND CONTROL DESIGN

A. Roll angle controllable region

We consider the *controllable region* of motorcycle systems (7) as the maximum roll angle region in which the system is possibly balanced around the vertical position ($\phi = 0$) for *any* given steering control design.

To make the analysis tractable, we assume that: (1) the tire/ground contact is a point rather than a patch; and (2) the two contact points C_1 and C_2 do not move (Fig. 1(c)). Under a roll angle ϕ, the lateral movement of the center of gravity G is approximated as $\Delta_{Gy} = h\sin\phi$. Now suppose that we apply a steering angle β on the front wheel, the turn of the front wheel will compensate for the lateral movement of point G by distance Δ_{Gy}^β as follows.

$$\Delta_{Gy}^\beta = \delta b\,\mathrm{c}_\phi = \frac{l_t b\,\mathrm{c}_\xi\,\mathrm{c}_\phi}{l}\beta_g. \tag{8}$$

To maintain the balance by steering, let $\Delta_{Gy} - \Delta_{Gy}^\beta = 0$ and thus we obtain

$$\phi = \tan^{-1}\left(\frac{b l_t\,\mathrm{c}_\xi}{hl}\beta_g\right). \tag{9}$$

For the Rutgers autonomous motorcycle, we use all physical parameters in Table I and $(\beta_g)_{\max} = \pi/3$ to obtain

$$\phi_{\max} = 4.4°.$$

Remark 1: From (9), we clearly see that the maximum stabilizable roll angle by steering depends on geometric parameters of the motorcycle system. Note that the analysis here is based on a simplified static and kinematic calculation and consideration of dynamic effects is ongoing work.

B. Domain of attraction (DOA)

We consider the DOA of the motorcycle dynamics (7) under a particular balance controller. We first specify a controller before analyzing DOA. Using a small angle approximation, we consider $\alpha \approx 0.05$ in the dynamics (7) and thus we rewrite (7) as

$$\ddot{\phi} = f_1(\phi) + f_2(\phi)\beta_g, \tag{10}$$

where

$$f_1(\phi) = \frac{mg\sin\phi}{I_x + mh^2}\left(h + \frac{0.05Rb}{l}\right) \quad \text{and}$$
$$f_2(\phi) = \frac{mgb\,\mathrm{c}_\phi}{(I_x + mh^2)l}\left[l_t\,\mathrm{c}_\xi - \frac{12R\xi}{\pi^2}\left(1 - \frac{\sqrt{3}}{2}\right)\right].$$

We design a sliding mode control for the dynamic systems (10). We first define a sliding surface $s = \phi + \lambda\dot{\phi}$. Then we design the controller

$$\beta_g = \frac{-\dot{\phi} - \lambda f_1(\phi) - Ks}{\lambda f_2(\phi)}, \tag{11}$$

where $\lambda > 0$ and $K > 0$ are constants. Plugging (11) into (10), we obtain

$$\ddot{\phi} = -\frac{K}{\lambda}\phi - \left(\frac{1}{\lambda} + K\right)\dot{\phi} \tag{12}$$

as the closed-loop dynamics.

To estimate DOA, we consider the case that the maximum projected steering angle is $\frac{\pi}{3}$, namely, $\beta_g \le \frac{\pi}{3}$. Combining (10) and (12), it is straightforward to obtain the DOA estimates given by

$$\left|\frac{-\frac{K}{\lambda}\phi - \left(\frac{1}{\lambda} + K\right)\dot{\phi} - f_1(\phi)}{f_2(\phi)}\right| \le \frac{\pi}{3}. \tag{13}$$

Fig. 4 shows the DOA estimates with three different sets of control parameters. It is interesting to find that when the controller is aggressive such as $K = 40$, the DOA becomes smaller. This is because that aggressive actions will increase the roll angular motion, which is undesirable for the balance control. Fig. 4 also shows that the DOA estimate under this type of sliding-mode control has a strip shape.

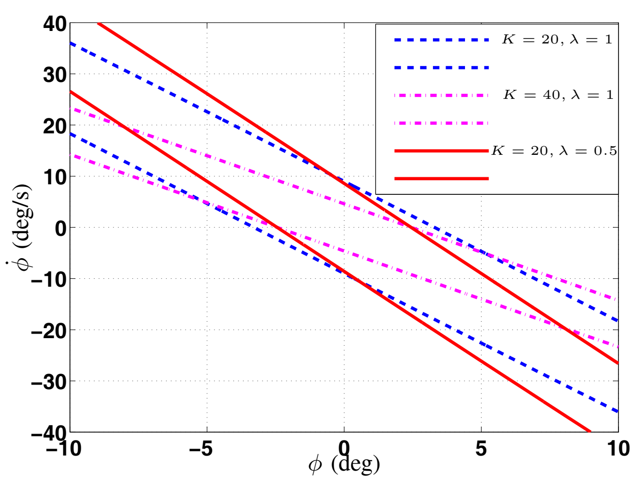

Fig. 4. DOA estimation under different sliding-mode control designs

IV. GPS/IMU-based Motorcycle Attitude Estimation

In the previous balance control analysis, we assume that we can measure the motorcycle attitude angles. It is not straightforward to obtain these measurements directly by onboard sensors. In this section, we present a novel GPS/IMU-based attitude estimation.

We define an inertial frame $\mathcal{I}(X, Y, Z)$ and a motorcycle body frame $\mathcal{B}(x, y, z)$ as shown in Fig. 1(b). Let $\mathbf{\Theta} := [\phi \;\; \theta \;\; \psi]^T$ denote the attitude angles, that is, the roll, pitch and yaw angles, respectively. The transformation from $\mathcal{I}$ to $\mathcal{B}$ is considered as the Z-Y-X ordered Euler angle rotation. The transformation relationship from frames $\mathcal{B}$ to $\mathcal{I}$ is [21]

$$C_B^I = \begin{bmatrix} \mathrm{c}_\theta\,\mathrm{c}_\psi & -\mathrm{s}_\psi\,\mathrm{c}_\phi + \mathrm{c}_\psi\,\mathrm{s}_\phi\,\mathrm{s}_\theta & \mathrm{s}_\phi\,\mathrm{s}_\psi + \mathrm{c}_\psi\,\mathrm{s}_\theta\,\mathrm{c}_\phi \\ \mathrm{c}_\theta\,\mathrm{s}_\psi & \mathrm{c}_\phi\,\mathrm{c}_\psi + \mathrm{s}_\theta\,\mathrm{s}_\phi\,\mathrm{s}_\psi & -\mathrm{s}_\phi\,\mathrm{c}_\psi + \mathrm{s}_\theta\,\mathrm{c}_\phi\,\mathrm{s}_\psi \\ -\mathrm{s}_\theta & \mathrm{c}_\theta\,\mathrm{s}_\phi & \mathrm{c}_\phi\,\mathrm{c}_\theta \end{bmatrix}.$$

Let $\mathbf{P}_I(t) \in \mathbb{R}^3$ and $\mathbf{V}_I(t) \in \mathbb{R}^3$ denote the position and velocity vectors of the IMU in $\mathcal{I}$, respectively. We denote the IMU acceleration and angular rate measurements in $\mathcal{B}$ as $\mathbf{A}_B = [a_{Bx} \;\; a_{By} \;\; a_{Bz}]^T \in \mathbb{R}^3$ and $\boldsymbol{\omega}_B = [\omega_{Bx} \;\; \omega_{By} \;\; \omega_{Bz}]^T \in \mathbb{R}^3$, respectively. We obtain the following kinematic motion equations for the IMU.

$$\dot{\mathbf{P}}_I = \mathbf{V}_I, \tag{14a}$$
$$\dot{\mathbf{V}}_I = C_B^I\mathbf{A}_B + \mathbf{G}, \tag{14b}$$
$$\dot{\phi} = \omega_{Bx} + s_\phi\tan\theta\omega_{By} + \mathrm{c}_\phi\tan\theta\omega_{Bz}, \tag{14c}$$
$$\dot{\theta} = \mathrm{c}_\phi\,\omega_{By} - \mathrm{s}_\phi\,\omega_{Bz}, \tag{14d}$$
$$\dot{\psi} = \frac{\mathrm{s}_\phi}{\mathrm{c}_\theta}\omega_{By} + \frac{\mathrm{c}_\phi}{\mathrm{c}_\theta}\omega_{Bz}, \tag{14e}$$

where $\mathbf{G} = [0 \;\; 0 \;\; -g]^T$.

We denote the GPS position in $\mathcal{I}$ as $\mathbf{P}_G \in \mathbb{R}^3$. From Fig. 1(b), we obtain

$$\mathbf{P}_G = \mathbf{P}_I + C_B^I\begin{bmatrix} b_p \\ 0 \\ h_p \end{bmatrix}, \tag{15}$$

where b_p and h_p are the horizontal and vertical distances between the GPS antenna and mass center G, respectively. Since the motorcycle does not have suspension, we consider the kinematic constraint of zero pitch angle, namely, $\theta = 0$. Therefore, we obtain the system output

$$\mathbf{y}(t) = [\mathbf{P}_G \;\; \theta]^T. \tag{16}$$

We define the state variable

$$\mathbf{X}(t) := \left[\mathbf{P}_I^T(t) \quad \mathbf{V}_I^T(t) \quad \mathbf{\Theta}^T(t)\right]^T \in \mathbb{R}^9$$

and re-write the kinematics (14) in a discrete-time form as

$$\mathbf{X}(k) = \mathbf{X}(k-1) + \Delta T\mathbf{f}\left(\mathbf{X}(k-1), \mathbf{u}(k-1)\right), \tag{17}$$

where $\mathbf{u}(k) := [\mathbf{A}_B^T(k) \;\; \boldsymbol{\omega}_B^T(k)]^T$ is the IMU measurements at the kth sampling time, ΔT is the data-sampling period. The function $\mathbf{f}\left(\mathbf{X}(k), \mathbf{u}(k)\right)$ is given in (14) as

$$\mathbf{f}\left(\mathbf{X}(k), \mathbf{u}(k)\right) = \begin{bmatrix} \mathbf{f}_P \\ \mathbf{f}_V \\ \mathbf{f}_\Theta \end{bmatrix} := \begin{bmatrix} \mathbf{V}_I(k) \\ C_B^I(k)\mathbf{A}_B(k) + \mathbf{G} \\ \mathbf{f}_\Theta(\mathbf{\Theta}(k), \boldsymbol{\omega}_B(k)) \end{bmatrix}, \tag{18}$$

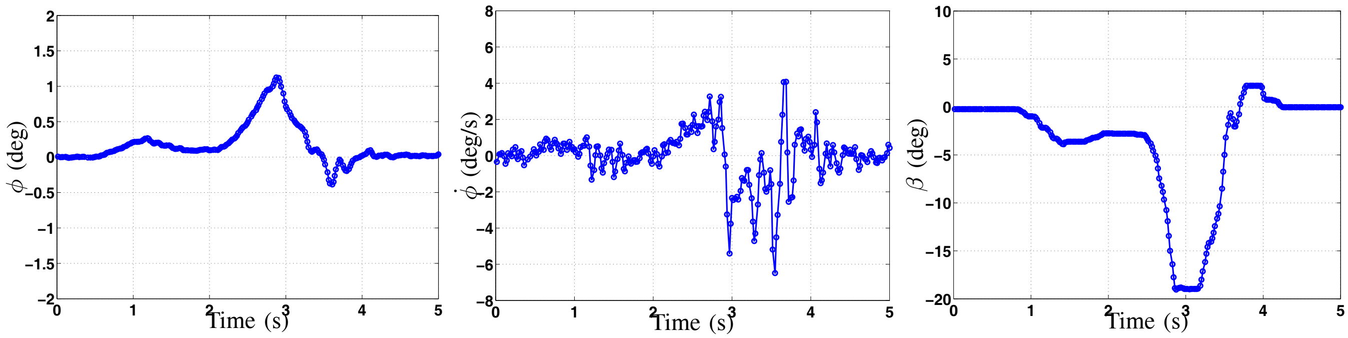

(a) (b) (c)

Fig. 5. Experimental results of the balance controller with $K = 20$ and $\lambda = 1$. (a) Roll angle ϕ. (b) Roll angle rate $\dot{\phi}$. (c) Steering angle β.

where $\mathbf{f}_P = \mathbf{V}_I(k)$, $\mathbf{f}_V = C_B^I \mathbf{A}_B(k) + \mathbf{G}$, and

$$\mathbf{f}_\Theta(\mathbf{\Theta}(k), \boldsymbol{\omega}_B(k)) := \begin{bmatrix} \omega_{Bx} + \tan\theta \left(\mathrm{s}_\phi \, \omega_{By} + \mathrm{c}_\phi \, \omega_{Bz} \right) \\ \mathrm{c}_\phi \, \omega_{By} - \mathrm{s}_\phi \, \omega_{Bz} \\ \frac{\mathrm{s}_\phi}{\mathrm{c}_\theta} \omega_{By} + \frac{\mathrm{c}_\phi}{\mathrm{c}_\theta} \omega_{Bz} \end{bmatrix}.$$

An EKF design is applied to the system (17) and (16). The details of EKF implementation are similar to those in [21] and we omit here due to the page limit.

V. Experiments

We conducted all experiments using the Rutgers autonomous motorcycle shown in Fig. 1(a). The stabilization controller and the EKF design are implemented on an onboard National Instruments (NI) CompactRIO real-time system. A MEMS-based low-cost IMU device (IMU605, MotionSense Inc.) provides the attitude rates and acceleration information at a sampling rate of 120 Hz. The GPS (Novetal RT2K, Novetal Inc.) gives the positioning information at a sampling rate of 20 Hz with a resolution of around 2 cm. The steering angle are measured by the encoder integrated with the steering motor. We use a set of cable potentiometers (Celesco SP1-25) to accurately provide the roll and yaw angle measurements for comparison purposes. In experiment, the rear tire is fully locked to achieve zero velocity constraint. The measured signals from various devices are integrated and synchronized through the CompactRIO's FPGA module.

The balance control experiments were conducted indoors and we used two cable potentiometers to provide the roll angle measurements in real time. Fig. 5 shows the experimental results. We introduced a disturbance roll angle (1.5 degs) to push motorcycle aside and the controller turned steering immediately. The motorcycle was then returned around the equilibrium position finally.

We now show a validation of the DOA estimation by two experiments. First, we set up a zero initial roll angular rate. The design parameters of the sliding-mode controller are $K = 20$ and $\lambda = 1$. By calculation, when $\dot{\phi} = 0$ we find the DOA boundary (e.g., curves in Fig. 4) is around 2.5 degs. In the first experiment, we use the motorized support jack to setup the motorcycle to start at 2.5 degs. In the second experiment, we set the initial roll angle to be slightly larger than 4 degs. Fig. 6 shows the experimental roll angle results. The results shown in Fig. 6 clearly illustrate that for the first experiment the controller can regulate the roll angle to return back to the equilibrium position, while in the second experiment, the motorcycle cannot be balanced and finally supported by the motorized jack. To protect the motorcycle from falling down, we set a 6-deg roll angle limit position by the support jack in experiments.

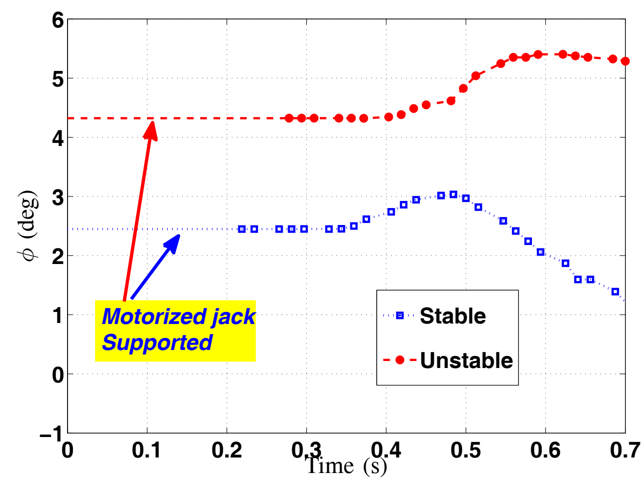

Fig. 6. Roll angle trajectory of experiments with two different initial roll angle values

We conducted and tested the EKF-based attitude estimation scheme on the Rutgers campus. We took the motorcycle outside the building on a campus parking plot. We manually swung the rear frame while at the same time turning steering mechanism. Fig. 7 shows the experimental results of the attitude angle estimates. The comparison results of roll, yaw and pitch angles are shown in Figs. 7(a)-7(c), respectively. The estimated roll and yaw angles are very close to the real values. It is also clear that the pitch angle is indeed around zero. For roll angle estimates, the maximum error is around 1.4 degs of a range of 15 degs. For yaw angle estimates, the maximum error is also around 1 deg for a range of 5 degs. The large maximum yaw angle estimation error is mainly due to that in experiments the potentiometer were connected to a flexible vertical plate installed on

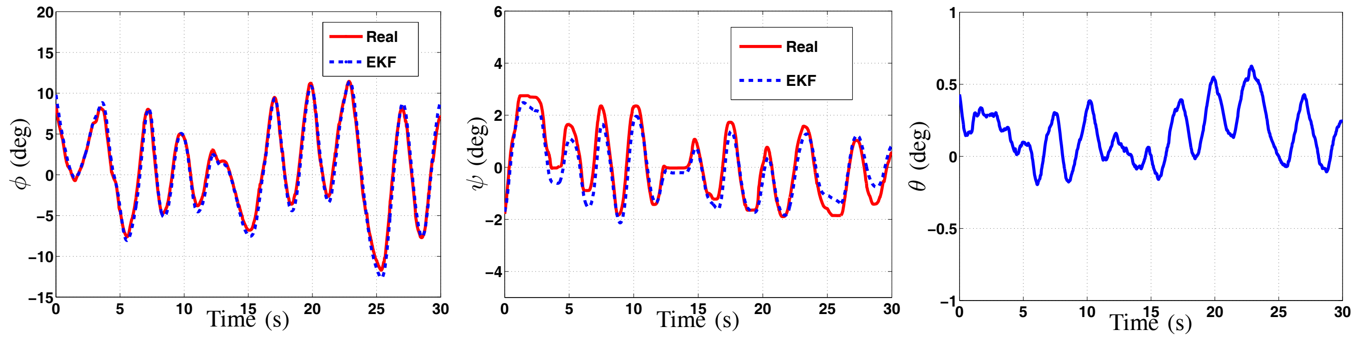

(a) (b) (c)

Fig. 7. Experimental results of the EKF-based attitude estimation. (a) Roll angle ϕ. (b) Yaw angle ψ. (c) Pitch angle θ.

the motorcycle. We have noticed that during experiments, the connected plate was deformed slightly and that could increase the measurement errors. These experimental results validate that the GPS/IMU-based attitude estimation scheme provides an effective way to obtain the motorcycle attitude in real time.

VI. Conclusion

We presented the balancing control analysis of a stationary riderless motorcycle system. We revealed geometric and kinematic relationship of the front wheel steering mechanism of the motorcycle system. We presented the analytical estimation of the domain of attraction (DOA) of the stationary motorcycle system. We found that only by steering, the DOA estimate is small and thus the balancing control of stationary motorcycle is challenging. We also discussed a GPS/IMU-based motorcycle attitude estimation scheme by using an EKF design with kinematic constraints. We implemented, tested and validated the balancing control design, DOA analysis, and the attitude estimation scheme on the Rutgers autonomous motorcycle. We are currently developing a more precise analysis of the DOA estimates. Extensively experimental testing of the analysis are also our ongoing work.

Acknowledgments

We thank Ms. Lesley Yu of the National Instruments Inc. for help and discussions. We also thank National Instruments Inc. for their generous equipment support (NI CompactRIO and various modules) for the project. We are grateful to the 2008/2009 Rutgers "Autonomous Motorcycle" senior design team for initially designing and building the testing platform.

References

[1] R. Sharp, "Stability, control and steering responses of motorcycles," *Veh. Syst. Dyn.*, vol. 35, no. 4-5, pp. 291–318, 2001.

[2] K. Åström, R. Klein, and A. Lennartsson, "Bicycle dynamics and control," *IEEE Control Syst. Mag.*, vol. 25, no. 4, pp. 26–47, 2005.

[3] D. Limebeer and R. Sharp, "Bicycles, motorcycles, and models," *IEEE Control Syst. Mag.*, vol. 26, no. 5, pp. 34–61, 2006.

[4] J. Lowell and H. McKell, "The stability of bicycles," *Amer. J. Phys.*, vol. 50, no. 12, pp. 1106–1112, 1982.

[5] R. Sharp, "The stability and control of motorcycles," *J. Mech. Eng. Sci.*, vol. 13, no. 5, pp. 316–329, 1971.

[6] N. Getz, "Dynamic inversion of nonlinear maps with applications to nonlinear control and robotics," Ph.D. dissertation, Dept. Electr. Eng. and Comp. Sci., Univ. Calif., Berkeley, CA, 1995.

[7] V. Cossalter and R. Lot, "A motorcycle multi-body model for real time simulations based on the natural coordinates approach," *Veh. Syst. Dyn.*, vol. 37, no. 6, pp. 423–447, 2002.

[8] V. Cossalter, *Motorcycle Dynamics*. Greendale, WI: Race Dynamics, 2002.

[9] T. Katayama, A. Aoki, and T. Nishimi, "Control behavior of motorcycle riders," *Veh. Syst. Dyn.*, vol. 17, no. 4, pp. 211–229, 1988.

[10] Y. Zhang and J. Yi, "Dynamic modeling and balance control of human/bicycle systems," in *Proc. IEEE/ASME Int. Conf. Adv. Intell. Mechatronics*, Montreal, Canada, 2010, pp. 1385–1390.

[11] V. Cossalter, R. Lot, and F. Maggio, "The modal analysis of a motorcycle in straight running and on a curve," *Meccanica*, vol. 39, pp. 1–16, 2004.

[12] J. Meijaard, J. Papadopoulos, A. Ruina, and A. Schwab, "Linearized dynamics equations for the balance and steer of a bicycle: A benchmark and review," *Proc. Royal Soc. A*, vol. 463, pp. 1955–1982, 2007.

[13] A. Beznos, A. Formal'sky, E. Gurfinkel, D. Jicharev, A. Lensky, K. Savitsky, and L. Tchesalin, "Control of autonomous motion of two-wheel bicycle with gyroscopic stabilisation," in *Proc. IEEE Int. Conf. Robot. Autom.*, Leuven, Belgium, 1998, pp. 2670–2675.

[14] S. Lee and W. Ham, "Self-stabilzing strategy in tracking control of unmanned electric bicycle with mass balance," in *Proc. IEEE/RSJ Int. Conf. Intell. Robot. Syst.*, Lausanne, Switzerland, 2002, pp. 2200–2205.

[15] J. Yi, D. Song, A. Levandowski, and S. Jayasuriya, "Trajectory tracking and balance stabilization control of autonomous motorcycles," in *Proc. IEEE Int. Conf. Robot. Autom.*, Orlando, FL, 2006, pp. 2583–2589.

[16] A. Levandowski, A. Schultz, C. Smart, A. Krasnov, H. Chau, B. Majusiak, F. Wang, D. Song, J. Yi, H. Lee, and A. Parish, "Ghostrider: Autonomous motorcycle," in *Proc. IEEE Int. Conf. Robot. Autom. (Video)*, Orlando, FL, 2006.

[17] Y. Tanaka and T. Murakami, "A study on straight-line tracking and posture control in electric bicycle," *IEEE Trans. Ind. Electron.*, vol. 56, no. 1, pp. 159–168, 2009.

[18] C.-G. Song, J.-Y. Kim, and N.-G. Kim, "A new postural balance control system for rehabilitation training based on virtual cycling," *IEEE Trans. Inform. Technol. Biomed.*, vol. 8, no. 2, pp. 200–207, 2004.

[19] B. Roy and H. H. Asada, "Nonlinear feedback control of a gravity-assisted underactuated manipulator with application to aircraft assembly," *IEEE Trans. Robotics*, vol. 25, no. 5, pp. 1125–1133, 2009.

[20] J. Yi, Y. Zhang, and D. Song, "Autonomous motorcycles for agile maneuvers: Part I: Dynamic modeling," in *Proc. IEEE Conf. Decision Control*, Shanghai, China, 2009, pp. 4613–4618.

[21] J. Yi, H. Wang, J. Zhang, D. Song, S. Jayasuriya, and J. Liu, "Kinematic modeling and analysis of skid-steered mobile robots with applications to low-cost inertial measurement unit-based motion estimation," *IEEE Trans. Robotics*, vol. 25, no. 5, pp. 1087–1097, 2009.